Monthly Notices
of the
ROYAL ASTRONOMICAL SOCIETY

MNRAS **450,** 3811–3821 (2015) doi:10.1093/mnras/stv834

GALEX catalogue of UV point sources in M33

Dale Mudd★ and K. Z. Stanek

Department of Astronomy, The Ohio State University, 140 W. 18th Ave, Columbus, OH 43210, USA

Accepted 2015 April 10. Received 2015 April 9; in original form 2014 June 27

ABSTRACT

The hottest stars (>10 000 K), and by extension typically the most massive ones, are those that will be prevalent in the ultraviolet (UV) portion of the electromagnetic spectrum, and we expect to numerous B, O and WR (WR) stars to be bright in UV data. In this paper, we update the previous point source UV catalogue of M33, created using the Ultraviolet Imaging Telescope (UIT), using data from the *Galaxy Evolution Explorer* (*GALEX*). We utilize point spread function photometry to optimally photometer sources in the crowded regions of the galaxy, and benefit from *GALEX*'s increased sensitivity compared to UIT. We match our detections with data from the Local Group Galaxies Survey to create a catalogue with photometry spanning from the far-UV through the optical for a final list of 24 738 sources. All of these sources have far-UV (FUV; 1516 Å), near-UV (NUV; 2267 Å) and *V* data, and a significant fraction also have *U*, *B*, *R* and *I* data as well. We also present an additional 3000 sources that have no matching optical counterpart. We compare all of our sources to a catalogue of known WR stars in M33 and find that we recover 114 of 206 stars with spatially-coincident UV point sources. Additionally, we highlight and investigate those sources with unique colours as well as a selection of other well-studied sources in M33.

Key words: catalogues – Local Group – ultraviolet: stars.

1 INTRODUCTION

M33, also known as the Triangulum Galaxy, was 'officially' discovered by Messier (1781), although it might have been noted more than a century earlier by Hodierno (1654). There is a wide range of calculated distances for this Local Group galaxy, ranging from 700 to 1100 kpc, and we adopt a distance of $d = 964$ kpc (Bonanos et al. 2006). Being so close, it is a well-studied galaxy indeed: as of 2015 April, the Astrophysics Data System reveals >1200 refereed papers with 'M33' in the abstract. M33 has been studied across many wavelengths (e.g. Warner, Wright & Baldwin 1973; Massey et al. 1996, 2006; Helfer et al. 2003; Pietsch et al. 2004; Thompson et al. 2009; Long et al. 2010) and across time (e.g. Hubble 1926; Hubble & Sandage 1953; Freedman, Wilson & Madore 1991; Macri, Sasselov & Stanek 2001; Hartman et al. 2006). Perhaps surprisingly, there have been relatively few studies of M33 in ultraviolet (UV) wavelengths (e.g. Massey et al. 1996; Thilker et al. 2005), and no catalogue of point sources based on *Galaxy Evolution Explorer* (*GALEX*) images of M33 has been published, a situation which we rectify in this paper.

The *GALEX* was launched in 2003. It was designed as a UV all-sky survey, with five smaller surveys making up the first portion of the mission. Specifically, we employ data from the Nearby Galaxy Survey (NGS) in the current work. The goal of the telescope was to gain a better understanding of galaxy evolution by studying local star formation, star formation histories, extinction and UV galaxy morphology (Martin & GALEX Science Team 2003). The instrument consisted of a 50 cm telescope connected to two sealed tube detectors and microchannel plates with a peak quantum efficiency of about 10 per cent. The dichroic splitter allowed for simultaneous observation in both the near- and far-UV (FUV) filters spanning from 1350 to 2800 Å. The circular field of view on the telescope had a diameter of roughly 1°.2. For more on the technical aspects of *GALEX*, see Jelinsky et al. (2003) and Morrissey et al. (2007).

A UV study of M33 is of potentially great importance. The most massive stars may appear quite faint in an optical survey since most of their emission may be concentrated in shorter wavelength bands. As such, a mission such as *GALEX* is ideal for identifying and characterizing these massive stars. Wolf–Rayet (WR) stars are also much more prominent in the UV with their extreme surface temperatures. In this work, we create a catalogue of UV point sources in M33 using the *GALEX* space telescope. We match this to a ground-based optical catalogue, as well as a list of known WR stars, in the galaxy and present photometric data spanning seven filters for tens of thousands of sources, which can be used for numerous astrophysical applications.

We begin by discussing the methods used for the construction of our catalogue and matching against the previous UV and optical catalogues of M33 in Section 2. In Section 3, we discuss the most interesting sources and aspects of our final product and then conclude.

★ E-mail: mudd@astronomy.ohio-state.edu

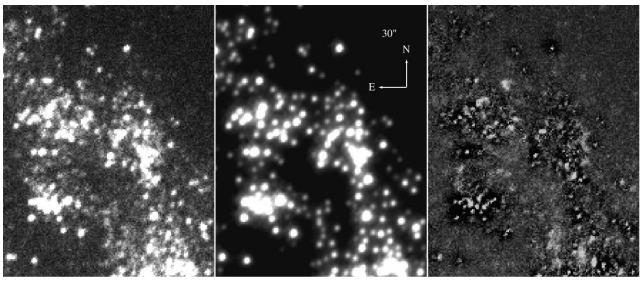

Figure 1. From left to right, the three panels are a fraction of a spiral arm from the original data, the sources detected, and the remaining flux after subtracting these sources using the derived PSF. The spatial scale is shown in the middle panel, where each line on the compass corresponds to 30 arcsec, as shown in the figure.

2 DATA AND METHODS

2.1 UV photometry

We begin with the UV science images[1] of M33 taken with the *GALEX* space telescope during the NGS on 2003 November 11. There are several pointings at M33 as part of *GALEX*'s survey. Tilings around the galaxy exist, but we opt to work with the central pointing of the galaxy since the photometric repeatability level of fainter sources, combining several tilings, could introduce errors of up to 0.4 mag (see Morrissey et al. 2007). The two exposures combine for a total exposure time of 3334 s. The simultaneous near-UV (NUV) and FUV images have passbands 1750–2800 Å and 1350–1750 Å and effective wavelengths of 2267 and 1516 Å, respectively. The point spread function (PSF) full width at half-maximum (FWHM) for the NUV and FUV detectors is 4.2 and 5.3 arcsec, respectively, sampled with 1.5 arcsec pixel^{-1}.

The D_{25}, the diameter at which the *B*-band surface brightness drops to 25 mag arcsec^{-2}, for M33 is 1°.2 (de Vaucouleurs et al. 1991), which corresponds well to the *GALEX* field of view. We began construction of our point source catalogue with the 'int' images from the *GALEX* pipeline, in units of counts per second corrected for effective exposure times, by performing PSF photometry with a combination of the DAOPHOT and ALLSTAR programs (Stetson 1987) on the NUV and FUV images separately. In our reduction, sources are required to have at least a 5σ detection with less than 0.3 mag in their uncertainty, and we begin by fitting sources with a purely analytic PSF for our baseline processing, a step that is strongly suggested for crowded sources as is the case with M33. A subset of the brightest and relatively isolated sources found under these conditions are then re-run through the reduction after subtracting out their nearest neighbours to iteratively improve the analytical PSF model empirically. In general, the empirical PSFs were slightly more elliptical than the analytic version. This refined PSF became the basis for our final source extraction. As an illustration, we show a comparison between the original image, the recovered stars, and the difference between the two in Fig. 1. From this figure, it is evident that many sources are successfully detected, but the limitation caused by the crowding in dense regions of the galaxy is readily apparent.

We then derived the necessary aperture correction on the brightest few hundred sources by using successively larger apertures (after subtracting out all other detected sources) and measuring the magnitude offsets between these and those measured with the final PSF model. For our aperture corrections, we found values of 0.03 mag for the FUV and 0.06 mag for the NUV. We next converted our instrumental magnitudes back to counts per second, which have been calibrated into both fluxes and AB magnitudes (Hayes & Latham 1975) by the GALEX Team (Morrissey et al. 2007). The AB magnitude system, in wavelength, is defined as

$$m_\nu = -2.5 \log \left(F_\lambda \times \frac{\lambda^2}{c} \right) - 48.60, \quad (1)$$

where flux F_λ is given in ergs^{-1} cm^{-2} Å^{-1}.

After applying the respective aperture corrections to the NUV and FUV catalogues and converting all sources to the AB system, we sought to match the FUV and NUV source catalogues. To do so while minimizing false matches, we began by matching using a 3 pixel maximum radius, or approximately 4.5 arcsec. As there were fewer sources in the FUV, we then kept only those sources with only one NUV match to a given FUV source within this radius. With this stringent cut of relatively large matching radius combined with only a single match, this list would contain a high concentration of correct source pairings. From these matches, we found the average offset between the NUV and FUV magnitudes (i.e. colours) and positions, along with the dispersion around these two values. These were then used to do a second round of matching the NUV to the FUV source list, keeping sources with more than a single counterpart in the NUV this time, based on minimizing the distance between objects in position–magnitude space with a maximum allowed physical separation of 2 pixels, or ∼3 arcsec. This resulted in a catalogue of 27 901 distinct *GALEX* FUV sources with NUV matches. Matching this way rather than through distance alone changed 209 total matches. Compared to the distance-only matches, our matches are of comparable separation, different by about 0.04 arcsec. However, they tend to be about 1 mag reduced in UV colour, which removed many strong colour outliers from the catalogue.

We then investigated the gross properties of our matches. We compare the source locations in the NUV to the FUV in Fig. 2. This gives us a sense of the spatial separation of our sources as well as their positional uncertainties, which are somewhat large. Fig. 3 shows the FUV luminosity function of our sources, which steadily rises until a turnover around 21 mag. Errors as a function of magnitude in both NUV and FUV are shown in Fig. 4 and a UV colour–magnitude diagram (CMD) is presented in Fig. 5.

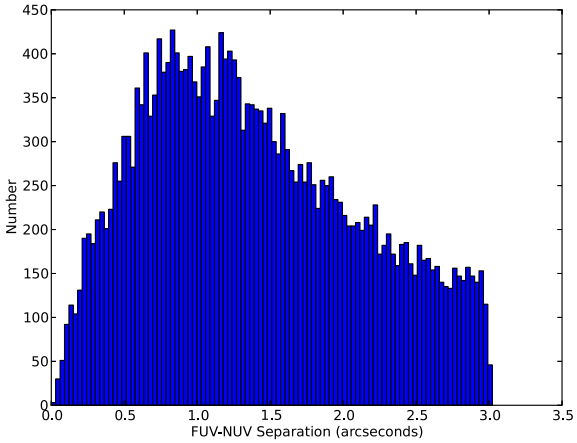

Figure 2. Histogram of the absolute separation, in arcseconds, between an FUV source and its corresponding NUV match.

[1] We retrieved these images from the Barbara A. Mikulski Archive for Space Telescopes (MAST).

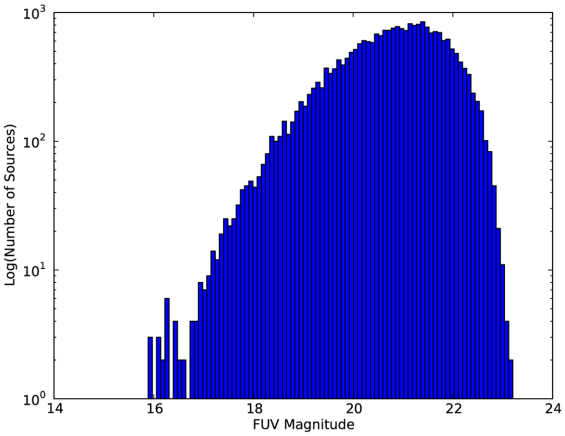

Figure 3. The FUV luminosity function of our final matched set of UV sources.

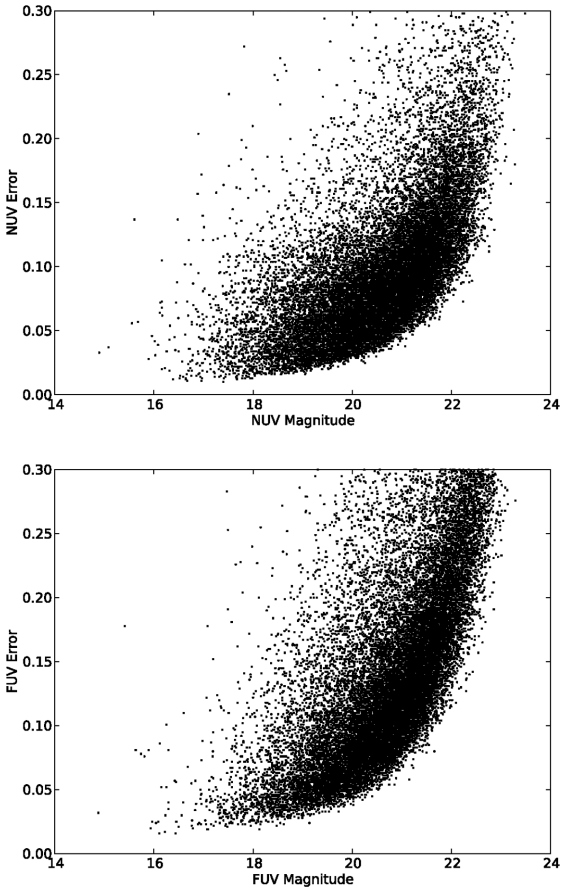

Figure 4. Error as a function of magnitude in the NUV (top) and FUV (bottom). As one might expect, the errors tend to grow for both filters for fainter sources.

Next, we compared our catalogue to the existing UV catalogue of M33 sources compiled in Massey et al. (1996). This catalogue was made using the Ultraviolet Imaging Telescope (UIT), an instrument aboard the *Astro-1* Mission (Stecher et al. 1992). UIT used photographic plates with the *B*1 and *A*1 filters roughly corresponding to the FUV and NUV filters of *GALEX*, having central wavelengths of ∼1500 and 2400 Å, respectively. It should be noted, however, that the *A*1 filter is significantly broader than the NUV filter on

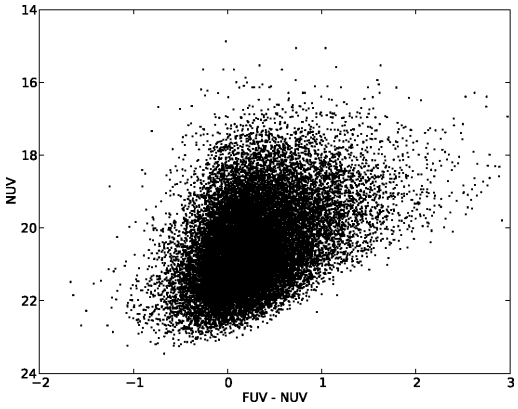

Figure 5. UV CMD of the final sources in our catalogue.

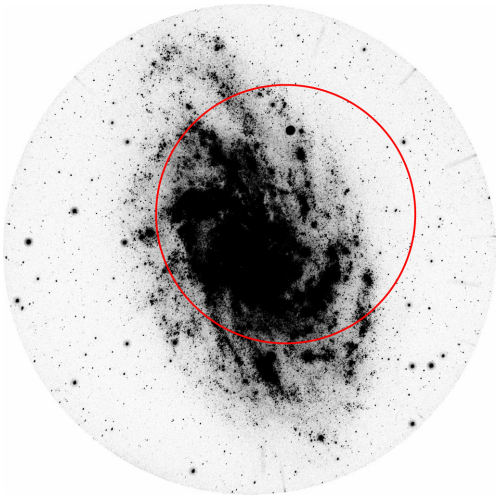

Figure 6. *GALEX* NUV image of M33. The inner circular region (radius of 18 arcmin) is the field of view of the UIT, used to create the previous UV point source catalogue for M33 (Massey et al. 1996).

GALEX, reaching several hundred angstroms to the red end of its *GALEX* counterpart. The field of view of UIT is also circular but has a smaller radius of 18 arcmin, which can be seen within the *GALEX* field of view in Fig. 6. The FWHM of UIT is comparable to that of *GALEX*, at 4 and 5.2 arcsec in the NUV and FUV filters, respectively. *GALEX*, however, reaps the reward of technological advancement over time in its implementation of more efficient microchannel plates instead of UIT's photographic ones. For more information on UIT and its detector's properties, see Stecher et al. (1992) and Landsman et al. (1992).

Similar to the analysis route we adopted, Massey et al. (1996) only keep sources for which there are both NUV and FUV detections, and they supplement these with *U*, *B*, and *V* ground-based data as well. Their final catalogue has 356 sources (note that the catalogue naming scheme goes as high as 374 as certain numbers are skipped), which they judge to be complete to an FUV AB magnitude of ∼18.5, corresponding to a specific flux of $F_{1500\,\text{Å}} = 2.5 \times 10^{-15}\,\text{erg cm}^{-2}\,\text{s}^{-1}\,\text{Å}^{-1}$, and its faintest source has an FUV magnitude of 19.7, corresponding to a specific flux of $F_{1500\,\text{Å}} = 6.4 \times 10^{-16}\,\text{erg cm}^{-2}\,\text{s}^{-1}\,\text{Å}^{-1}$. The *GALEX* observations are much more sensitive, and over 20 000 of our sources are fainter than this, a difference that is highlighted in Fig. 7. The faintest source in our final catalogue has an FUV magnitude of 23.3, corresponding to a specific flux of $F_{1500\,\text{Å}} = 2.3 \times 10^{-17}\,\text{erg cm}^{-2}\,\text{s}^{-1}\,\text{Å}^{-1}$.

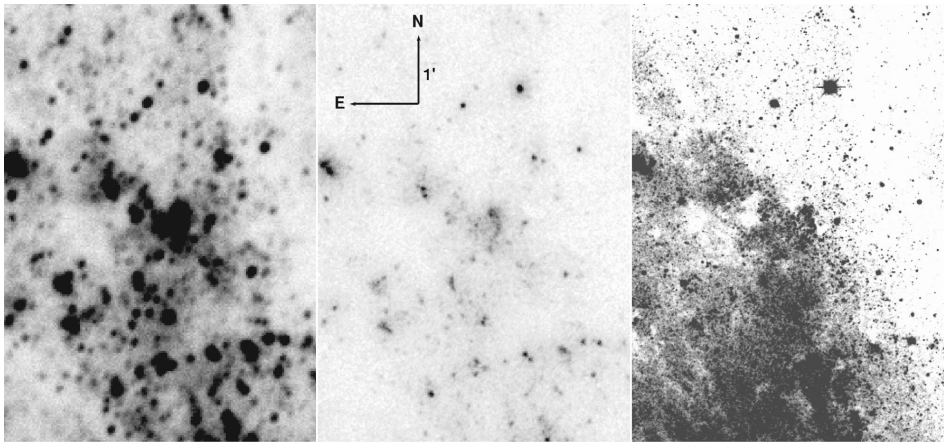

Figure 7. Comparison of a region in M33 with *GALEX* (left), UIT (middle) and *V*-band from the LGGS with the Mayall 4 m telescope (right; Massey et al. 2006). The two UV instruments have similar full width at half-maxima (∼4 arcsec), while *GALEX* has much greater sensitivity. The sides of the compass in the middle figure correspond to a size on the sky of 1 arcmin. The optical image highlights the problem of crowding that is prevalent throughout the UV data.

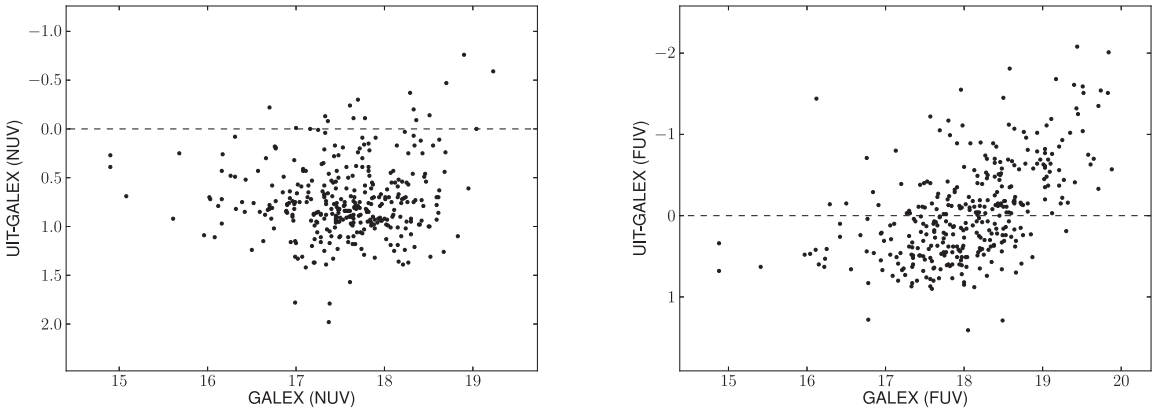

Figure 8. AB magnitude difference between UIT (Massey et al. 1996) and our *GALEX* catalogue as a function of *GALEX* NUV (left) and FUV (right) magnitude.

Looking at the astrometry solution for *GALEX*, we found there were some slight distortions in the two images, especially near the edges of the galaxy. We use the astrometry.net World Coordinate System (WCS) solution for our field (Lang et al. 2012) to correct this.[2] As the FUV image does not have enough sources outside the galaxy to find a solution, we apply the solution for the NUV image to the FUV one as well. Similar to the procedure followed for matching our NUV and FUV sources internally, we matched to the UIT catalogue, this time with a radius of 3.2 arcsec to complement our previous maximum radius, cut to those sources for which there was only a single UIT star within this radius, and then found the average and standard deviation for the magnitude and position offsets between the two catalogues. After this, we rematched based on magnitude and position once again. The distribution of matches by separation is shown in Fig. 9. From this, we decided to stick with a maximum radial separation of 3.2 arcsec as before. The remaining sources making this cut had a right ascension and declination offsets (UIT−*GALEX*) of 0.17 arcsec and −0.08 arcsec, respectively. Both of these are quite small compared to the size of the PSF.

This final catalogue had 348 sources in common with the original UIT catalogue of M33, which contained 356 sources. The average difference between NUV magnitudes (UIT−*GALEX*) is 0.73 mag with a spread of 0.38. For the FUV filters, the same calculation gives an offset of −0.04 mag and a dispersion of 0.60. These offsets as a function of magnitude in both NUV and FUV are shown in Fig. 8. While the NUV has a large offset, it does not appear to have any structure in it, whereas the FUV shows a trend of the *GALEX* photometry of faint sources being systematically fainter than in the original catalogue. Looking at the eight sources that we did not recover, seven of them were in crowded regions separated into sources by our PSF photometry differently than UIT such that the UIT object had several potential *GALEX* matches surrounding it, but none were within the matching radius. The final source, [MBH96] 167, is in a more diffuse, fainter region and it is surprising that it does not appear in our catalogue given that *GALEX* has a higher sensitivity than UIT. We investigate our raw photometry and the images themselves and found this object appears in both of the images and in the initial FUV photometry but was not selected as an NUV source and hence did not make it into our catalogue.

We inspected by eye many of the sources with the largest discrepancies in magnitude (Δ mag>1) in either band between the UIT and our catalogue. The largest offsets in the FUV were typically sources that were in crowded regions that were split into

[2] These images with the new WCS solutions can be found at http://www.astronomy.ohio-state.edu/∼mudd/gallery.html.

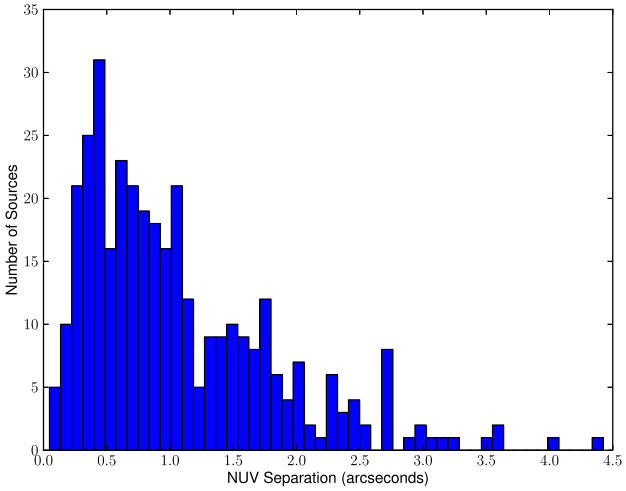

Figure 9. Distribution of matches between UIT (Massey et al. 1996) and our *GALEX* catalogue as a function of source separation in the NUV bands.

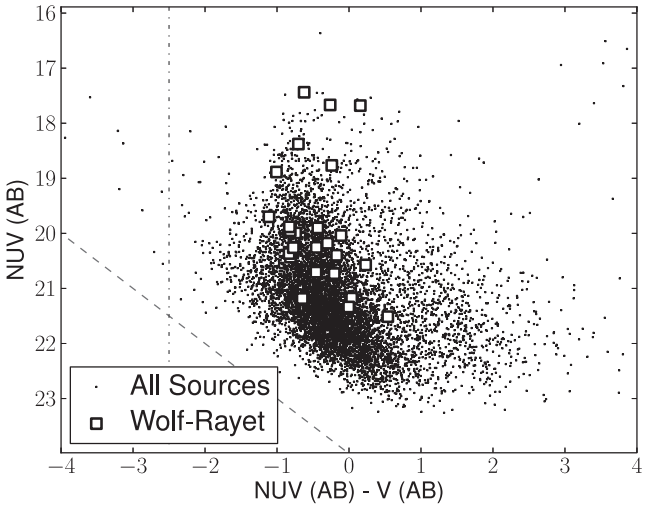

Figure 10. CMD (NUV−*V*) for *GALEX* matches to those sources found in the LGGS (Massey et al. 2006), where only a single optical counterpart was found within 3.2 arcsec (5032 sources). The red dashed line is the approximate magnitude cutoff of the optical study ($V = 24$), whereas the blue vertical dot–dashed line is the bluest a blackbody can be if both the NUV and *V* fluxes lie on the Rayleigh–Jeans tail of a blackbody. The squares represent the 25 WR stars, taken from Neugent & Massey (2011), that have only a single counterpart.

several sources in *GALEX* and tended to be brighter in UIT, as one might expect. The largest offsets in the NUV, however, were all brighter in our catalogue. Most of these were in more diffuse or isolated regions compared to the more clustered FUV-discrepant sources. There were a total of 65, 30 sources differing by more than a magnitude in the NUV and FUV, respectively.

To test for any systematic separation between our magnitudes and those from Massey et al. (1996) due to differences in the filter shapes of UIT and *GALEX*, we applied the four filter curves (UIT *A*1, *B*1 and *GALEX* FUV, NUV) to various temperature black bodies to estimate what the magnitude separation would be between UIT and *GALEX*. The FUV filters for the two instruments are quite similar, and, as such, the magnitude difference for a 40 000 K blackbody (UIT − *GALEX*), a temperature equivalent to a warm O star, was −0.02, which is quite close to the average offset we reported above. For the NUV, however, the 40 000 K blackbody has a magnitude difference (again, UIT − *GALEX*) of 0.17, which does not fully account for the average NUV offset we find. The exact cause of this offset remains unclear. Given the extensive testing of the *GALEX* detectors (see again Morrissey et al. 2007), however, we are more inclined to trust the new UV magnitudes of the sources presented here.

The UIT catalogue, with both the original and newly-derived *GALEX* parameter values (when available), is presented in Table 1.

2.2 UV–optical catalogue

Having completed our update of the UIT catalogue of known M33 UV sources with *GALEX* photometry, we next set out to expand on this with our additional ∼25 000 sources. To this end, we combine our UV sources with optical counterparts found in a similar-depth study of M33 in *U*, *B*, *V*, *R* and *I* from the Local Group Galaxies Survey (LGGS; Massey et al. 2006).

First, we matched our *GALEX* catalogue to the LGGS catalogue with our previous matching radius of 3.2 arcsec. As before, to get an idea of what unique physical matches look like, we investigated those sources that only had a single optical counterpart within the matching radius. This informed us of the true sky separations and colours we might expect from all real matches, since these sources are relatively isolated and there will be little confusion in any matching for them. These single matches are shown in Fig. 10. Of special note is the blue vertical line in the figure. This represents approximately the bluest colour a blackbody can have (NUV − $V = -2.5$), assuming both the NUV and *V* data lie on the Rayleigh–Jeans tail on the red side of the Wien Law peak. Stars can, of course, get around this via emission and absorption, but it is illustrative to know what fraction of our sources are 'unphysically' blue. In this subsample, we find that only 0.1 per cent of our pairs are bluer than this line. The average colour (NUV−*V*) of all our unique-matched sources is −0.09, but the dispersion is not surprisingly high, given the wealth of different stars we are probing, at 0.82.

Table 1. UIT sources that were recovered using *GALEX* data. Here, 'Matches' refers to the number of *GALEX* objects we find that are within 5 arcsec and compatible with the given UIT source. The subscript 'U' stands for UIT, whereas the subscript 'G' stands for *GALEX*. The first five sources are given to show the formatting. The full version of this table is available in the online version.

			GALEX photometry of [MBH96] sources									
UIT	α_U	δ_U	α_G	δ_G	FUV_U	NUV_U	FUV_G	NUV_G	FUV_{U-G}	NUV_{U-G}	Sep(arcsec)	Matches
2	23.133 00	30.582 75	23.133 35	30.582 62	18.19	18.31	18.03 ± 0.06	17.62 ± 0.03	0.09	0.69	1.18	3
3	23.157 08	30.668 25	23.156 77	30.668 29	17.44	17.35	17.59 ± 0.08	16.86 ± 0.02	0.01	0.49	0.97	2
4	23.158 54	30.667 97	23.158 13	30.668 10	17.70	18.31	17.69 ± 0.06	17.48 ± 0.03	− 0.94	0.83	1.35	1
5	23.178 71	30.646 44	23.178 55	30.646 42	18.15	17.84	18.26 ± 0.15	16.96 ± 0.01	1.37	0.88	0.5	2
6	23.185 83	30.583 25	23.185 97	30.583 33	17.67	17.93	17.80 ± 0.09	17.40 ± 0.08	− 0.35	0.53	0.52	2

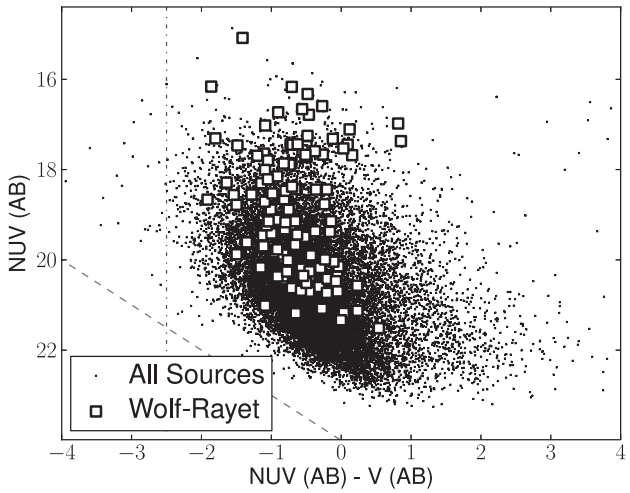

Figure 11. Final CMD (NUV−*V*) for *GALEX* matches to those sources found in Massey et al. (2006) (24 738 sources, 114 WR stars). The red and blue lines as well as the large squares are the same as those in Fig. 10. See Section 2.2 for a description of the criteria applied to find these matches.

Enlightened by our clean, 1:1 sample, we then iteratively refined our matching algorithm, i.e. combinations of colours and positional offsets, to determine our final matches. We expected that a successfully matched paired catalogue would have similar properties to that shown in Fig. 10. The final catalogue is matched based around a standard deviation of position of 1.2 arcsec, with a maximum allowed separation of 3.2 arcsec, and standard deviation of NUV − *V* colour of 0.8. The full matched CMD is shown in Fig. 11. We note that it is bluer on average than the clean sample at −0.42 mag with a median of −0.45 mag, has slightly lower dispersion, and the same fraction of 'too blue' stars.

Investigating some of the brightest of these 'too blue' sources, a pattern emerges. The brightest of these are all surrounding bright foreground objects and are thus likely being affected by image processing artefacts and their proximity to these extremely bright stars. The rest appear to cluster in a single dense region of the galaxy, the H II region NGC 604.

Our final catalogue, with data spanning 1516–7980 Å for most stars, is provided in Table 2 and has a total of 24 738 sources. Note that the catalogue has been constructed in such a way that each detected FUV source appears only once, but that each optical source has the freedom to match to more than one FUV source. When this happens, we report all the separate UV sources that have each given optical star as its best match. The average number of optical matches to a given UV source is 2.75 with a maximum of 20. The average positional offset between UV and *V* coordinates is 1.25 arcsec with a standard deviation of 074 arcsec. These are both smaller than the FWHM of the *GALEX* detector. We also calculate approximate luminosities in each band by using the effective wavelengths of each filter, the *GALEX* calibrations for the NUV and FUV flux zero-points and optical zero-points taken from Bessell, Castelli & Plez (1998), and the distance to M33 adopted from Bonanos et al. (2006). Sources without a matching optical counterpart are provided in Table 3.

3 DISCUSSION

With our UV/optical catalogue in hand, we next investigate a selection of the more well-known stars in M33 that are likely also

Table 2. Our UV sources that had optical counterparts from the LGGS. Note that all magnitudes are in the AB system. Here, 'Matches' refers to the number of optical objects we find that are within 3.2 arcsec of the *GALEX* source. Note that 'Sep' refers to the absolute separation between the object's position in the UV and optical catalogues. The full version of this table is available in the online version.

Full catalogue																					
Name	α_{UV}	δ_{UV}	α_{Opt}	δ_{Opt}	FUV	err_F	NUV	err_F	*U*	err_U	*B*	err_B	*V*	err_V	*R*	err_R	*I*	err_I	Sep(arcsec)	Matches
J013239.46+301952.5	23.164 39	30.331 69	23.164 42	30.331 25	21.869	0.127	21.862	0.115	22.229	0.021	22.227	0.032	22.608	0.051	22.677	0.1	99.999	99.999	1.587	1
J013239.45+302241.6	23.164 30	30.378 32	23.164 37	30.378 22	20.082	0.056	20.157	0.041	20.425	0.004	20.616	0.009	20.891	0.013	21.049	0.012	21.284	0.004	0.421	2
J013239.46+303955.1	23.164 13	30.665 41	23.164 42	30.665 31	20.340	0.087	19.884	0.037	20.063	0.004	20.225	0.006	20.503	0.008	20.79	0.01	21.121	0.0	0.967	1
J013354.22+304410.5	23.475 61	30.736 63	23.475 92	30.736 25	20.536	0.179	20.303	0.198	19.766	0.003	19.968	0.006	20.257	0.009	20.492	0.011	20.712	0.0	1.671	2
J013239.45+302214.4	23.164 48	30.370 81	23.164 37	30.370 67	20.438	0.061	20.514	0.061	20.563	0.005	20.623	0.012	20.858	0.012	21.114	0.016	21.456	0.0	0.609	1
J013349.96+304323.4	23.458 09	30.722 94	23.458 17	30.723 17	20.662	0.183	19.763	0.058	21.578	0.02	21.149	0.025	21.271	0.03	20.975	0.023	20.17	0.0	0.864	3
J013349.96+305256.2	23.458 45	30.882 62	23.458 17	30.882 28	18.714	0.093	18.665	0.037	19.546	0.014	19.684	0.01	19.904	0.014	19.947	0.017	20.059	0.001	1.499	4
J013349.96+305256.2	23.458 45	30.882 62	23.458 17	30.882 28	20.451	0.104	18.665	0.037	19.546	0.014	19.684	0.01	19.904	0.014	19.947	0.017	20.059	0.001	1.499	4
J013349.96+303427.8	23.458 01	30.574 27	23.458 17	30.574 39	20.638	0.083	20.541	0.083	20.6	0.004	20.821	0.011	21.138	0.014	21.45	0.019	21.743	0.0	0.658	2
J013321.23+304042.0	23.338 14	30.678 49	23.338 46	30.678 33	20.676	0.084	20.413	0.058	20.678	0.006	20.563	0.009	20.921	0.013	21.236	0.015	21.665	0.0	1.146	2
J013358.39+304823.7	23.493 06	30.806 83	23.493 29	30.806 58	20.493	0.122	20.091	0.044	20.702	0.006	20.674	0.011	20.905	0.014	21.1	0.018	21.386	0.0	1.147	2

Table 3. Those UV sources that did not have an optical counterpart. Here, $N_{\rm mat}$ refers to the number of NUV sources within 3.2 arcsec of the FUV source. The full version of this table is provided in the online version.

ID	$\alpha_{\rm UV}$	$\delta_{\rm UV}$	FUV	NUV	$N_{\rm mat}$
6	23.624 97	30.107 37	15.713 ± 0.022	16.135 ± 0.02	2
363	22.945 42	30.367 58	17.978 ± 0.035	16.992 ± 0.132	2
396	23.677 46	30.424 22	18.039 ± 0.062	14.314 ± 0.026	1
525	24.095 94	30.671 27	18.213 ± 0.043	15.853 ± 0.022	2
711	23.963 06	30.324 53	18.38 ± 0.045	15.622 ± 0.015	1
759	23.000 21	30.365 43	18.413 ± 0.041	15.022 ± 0.036	1

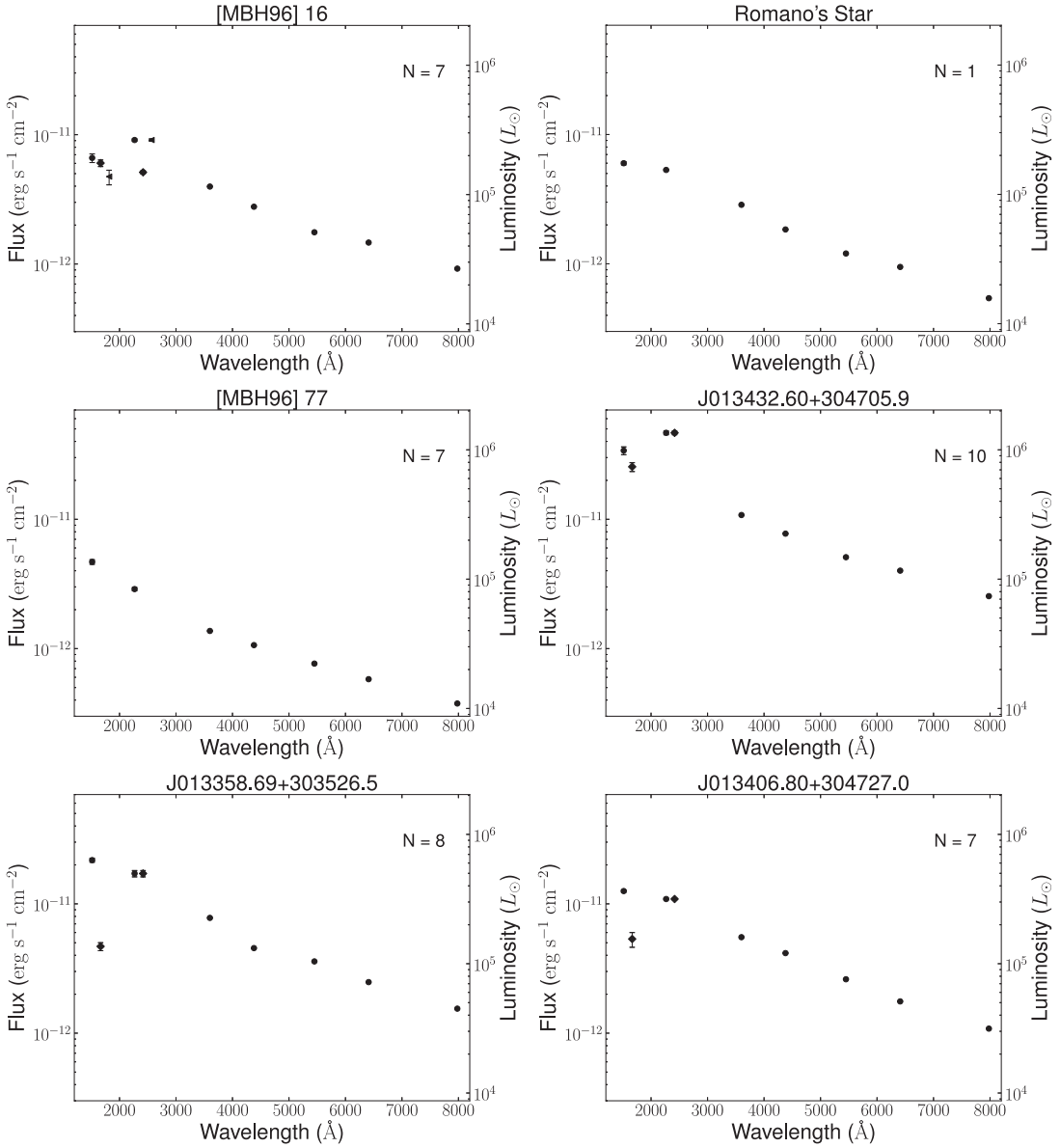

Figure 12. A selection of some of the UV-brightest and most well-studied WR stars in M33 that are in the final catalogue. First row: [MBH96] 16 (left) and Romano's Star (right). Second row: [MBH96] 77 (left) and J013432.60+304705.9 (right). Third row: LGGS J013358.69+303526.5 (left) and J013406.80+304727.0 (right). In the top-right corner of each panel, the value '*N*' corresponds to the number of optical sources that were within 3.2 arcsec of the UV source and is provided as a measure of crowding, which tended to be most severe for the few hundred brightest of the UV sources. In the cases where there are multiple UV sources with a given optical star as its best match, the value given for '*N*' is the average amongst these sources. For a description of the matching process, see Section 2.2.

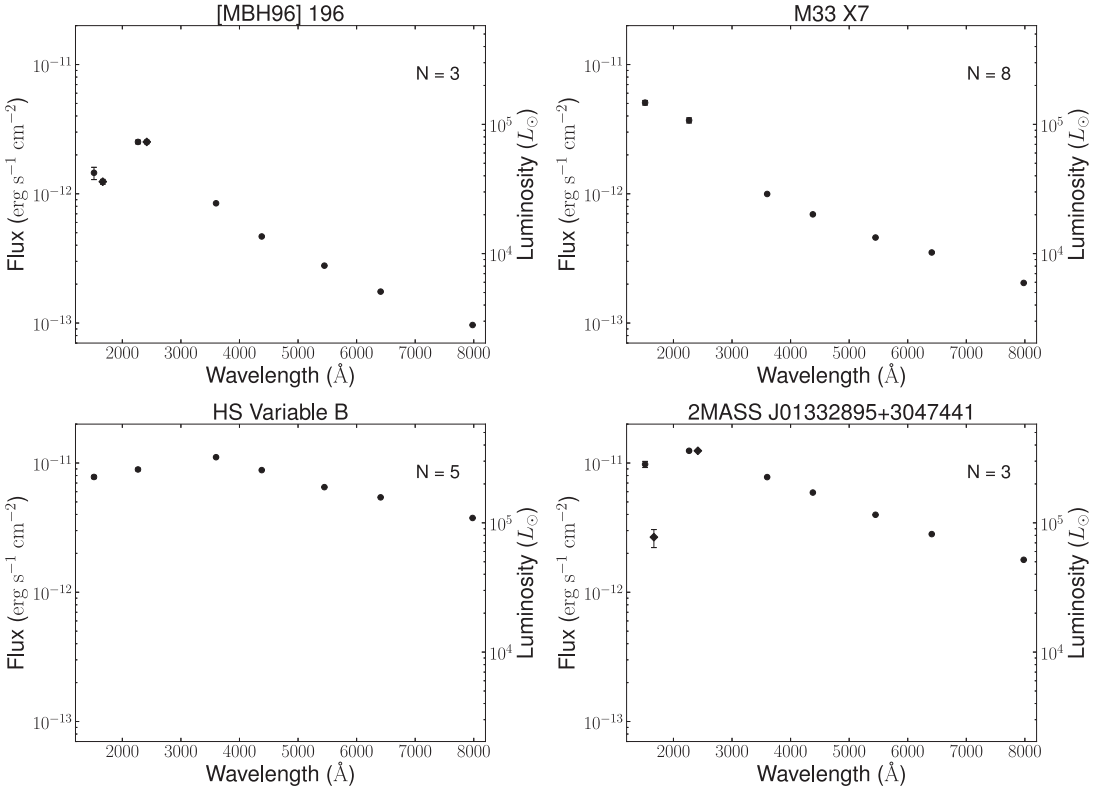

Figure 13. Same as Fig. 12 but for other, non-WR sources in M33. First row: [MBH96] 196, a detached eclipsing binary that has been used to measure the distance to M33, and M33 X-7 (HMXB). Second row: Hubble–Sandage Variable B (left) and 2MASS J01332895+3047441, both blue supergiants.

UV bright. First, we look at a selection of WRs, thought to be massive (>20 $M_\odot$) stars that have blown off their envelopes and have become essentially hot, exposed stellar cores. With effective temperatures typically in excess of 30 000 K, occasionally reaching well over 100 000 K, these stars should peak at a wavelength bluewards of even *GALEX*'s FUV filter. As such, ignoring any absorption or extinction, we expect these stars to be among the highest luminosity in the FUV from the bandpasses presented here. In Fig. 12, the sources [MBH96] 16, Romano's Star (Romano 1978) and [MBH96] 77, presented in the top and middle rows, are a selection of the most well-known WR stars in the galaxy. [MBH96] 16, as can be seen from the figure, has three separate UV matches to its optical counterpart in our data. Two of these peak in the NUV, whereas one continues to rise in the FUV. Since it is a WR star, the most likely true match is this hottest UV source. Romano's Star, [MBH96] 77, LGGS J013358.69+303526.5 and LGGS J013406.80+304727.0 also exhibit this behaviour, albeit with somewhat different slopes. Comparing our sources to a catalogue of known WR stars in M33 (Neugent & Massey 2011), we recover 114 out of a total 206.

Another star we investigate is a detached eclipsing binary used by the DIRECT Project (Bonanos et al. 2006) to measure the distance to M33 itself, whose SED is presented in Fig. 13. The two stars in this binary have derived temperatures in excess of 35 000 K. Our best matches, however, peak in the NUV rather than the FUV, as one might expect. Next, we look at M33 X-7 (e.g. Long et al. 1981, 2010), a high-mass X-ray binary. From Fig. 13, we see that it is quite luminous in the UV bands, as might be predicted due to the presence of both an accreting compact object and a hot stellar companion. We also have a number of well-studied blue supergiants in our sample, including Hubble–Sandage Variable B (Hubble & Sandage 1953) and 2MASS J01332895+3047441 (Kunchev & Ivanov 1986; Ivanov, Freedman & Madore 1993; Skrutskie et al. 2006). These stars, although blue, are much cooler than WR stars and we anticipate their spectral energy distributions to peak at longer wavelengths. Both matches to 2MASS J01332895+3047441 peak in the NUV. This star has been classified as a B-type supergiant (Massey et al. 2006), which can indeed be warm enough to peak bluewards of the optical range.

After searching the catalogue for known interesting sources, an obvious next step is to look at the luminous stars in the catalogue. We present the six most luminous sources in Fig. 14, where 'most luminous' here is defined as the summation of fluxes from all available bands. Immediately a trend appears. All of these stars have most of their flux in the optical bandpasses and the UV data contributes minimally to their total bolometric luminosity. The brightest stars in the catalogue, then, are likely all relatively common and cooler red supergiants, though there may be also some of the rarer yet more intrinsically luminous yellow supergiants, as well as a few foreground sources.

For which stars does the UV data significantly change their inferred bolometric luminosities? To answer this question, we present the six stars with the highest luminosity in *GALEX*'s FUV bandpass in Fig. 15. Three of these were found in the UIT catalogue of M33, but three are new UV sources. All of these tend to have NUV and FUV luminosities of around 10^6 $L_\odot$. This is a factor of 6 down from the peak bandpass luminosity in Fig. 14, but it is of the same order of magnitude as in those stars. The difference is that the UV bright stars are bright solely in the UV, often dropping by at least a factor of 2 in flux between the NUV and *V*-bands. And this is not unexpected of extremely hot stars which will emit

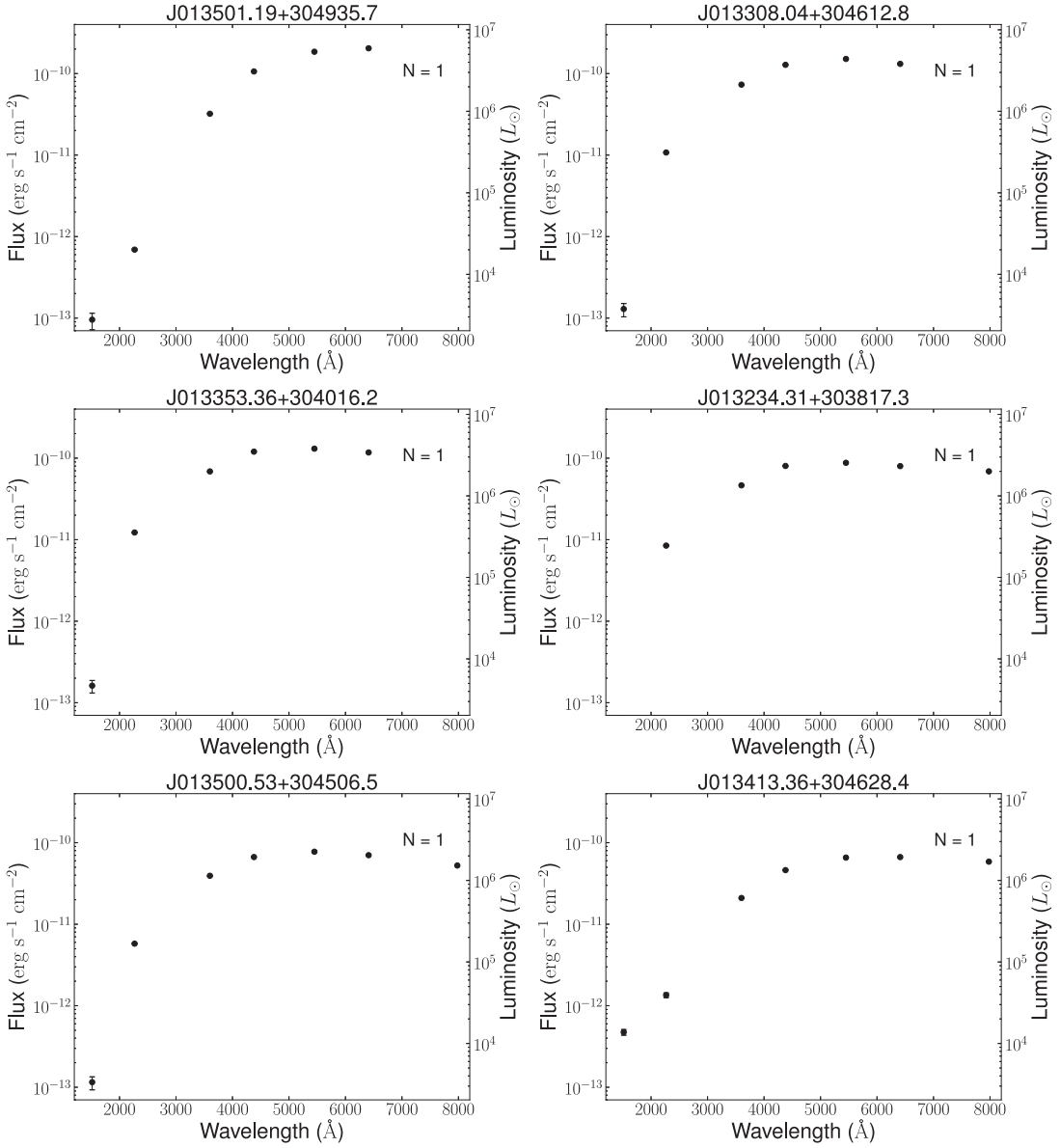

Figure 14. Same as Fig. 12 but for the six most luminous stars in the catalogue (combination of all bands).

significantly in the UV but have their flux fall continually in redder bands.

With this work, we seek to update and expand the existing UV catalogue of M33 using archival *GALEX* data. Using PSF photometry to optimally find and photometer sources, we find tens of thousands of more sources than in the pipeline product as it was not constructed to handle such a crowded environment. We match these to the UIT catalogue (Massey et al. 1996) and recover all but eight of these sources. Next, we match to an optical catalogue from the LGGS (Massey et al. 2006) to create a final catalogue with 27 901 sources, of which 24 738 have optical matches thereby spanning seven filters from the FUV to near-IR. We then investigate the properties of our catalogue and find that the most overall luminous sources are typically brightest in the optical bands (and hence likely evolved stars), but there are still many sources, likely young, massive stars and WR stars, that are continuing to rise in the UV range, indicating high effective temperatures.

A useful future endeavour would be to perform a similar analysis with the *Swift* UV data of M33 (Immler & Swift Satellite Team 2008). *Swift* covers three UV filters with high spatial resolution, which would further assist in lessening the obvious crowding issue that is persistent in both the *GALEX* and UIT data.

ACKNOWLEDGEMENTS

DM would like to thank Philip Massey, Scott Adams, Michael Fausnaugh, Rubab Khan, Ben Shappee and Obright Lorain for helpful discussions that contributed greatly to this paper. We also wish to thank the anonymous referee, who provided numerous useful comments and aided the betterment of this manuscript.

Based on observations made with the NASA *GALEX*. Some of the data presented in this paper were obtained from the Mikulski Archive for Space Telescopes (MAST). STScI is operated by the Association of Universities for Research in Astronomy, Inc.,

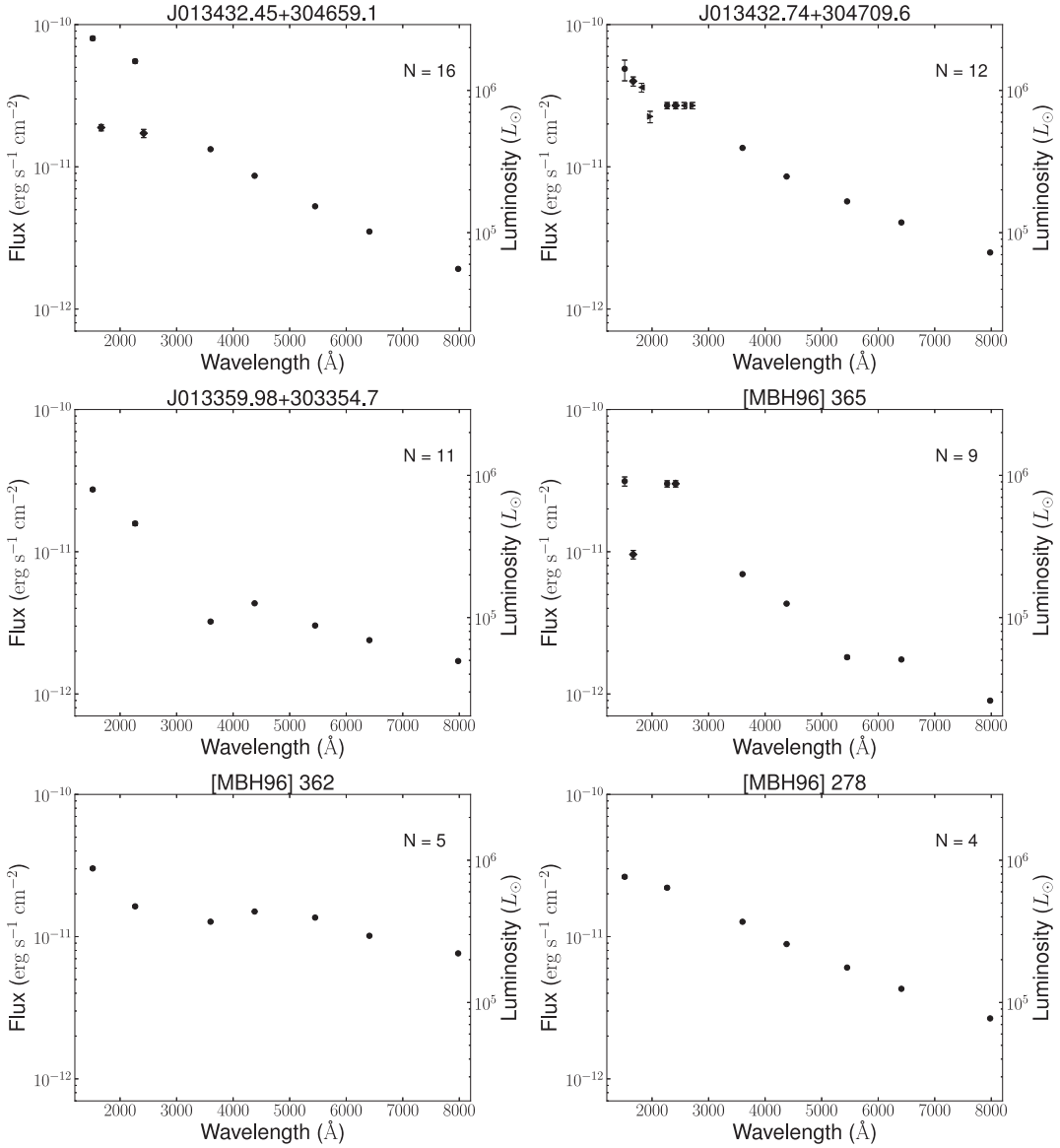

Figure 15. Same as Fig. 12 but for the six stars with the highest UV luminosity in the catalogue. We note that the UV brightest stars also tend to be the most crowded, as is evident from the large values of '*N*'.

under NASA contract NAS5-26555. Support for MAST for non-HST data is provided by the NASA Office of Space Science via grant NNX13AC07G and by other grants and contracts. Some/all of the data presented in this paper were obtained from the Mikulski Archive for Space Telescopes (MAST). STScI is operated by the Association of Universities for Research in Astronomy, Inc., under NASA contract NAS5-26555. Support for MAST for non-HST data is provided by the NASA Office of Space Science via grant NNX09AF08G and by other grants and contracts.

REFERENCES

Bessell M. S., Castelli F., Plez B., 1998, A&A, 333, 231
Bonanos A. Z. et al., 2006, ApJ, 652, 313
de Vaucouleurs G., de Vaucouleurs A., Corwin H. G., Jr., Buta R. J., Paturel G., Fouqué P., 1991, Third Reference Catalogue of Bright Galaxies. Volume I: Explanations and references. Volume II: Data for galaxies between 0^h and 12^h. Volume III: Data for galaxies between 12^h and 24^h. Springer, New York
Freedman W. L., Wilson C. D., Madore B. F., 1991, ApJ, 372, 455
Hartman J. D., Bersier D., Stanek K. Z., Beaulieu J.-P., Kaluzny J., Marquette J.-B., Stetson P. B., Schwarzenberg-Czerny A., 2006, MNRAS, 371, 1405
Hayes D. S., Latham D. W., 1975, ApJ, 197, 593
Helfer T. T., Thornley M. D., Regan M. W., Wong T., Sheth K., Vogel S. N., Blitz L., Bock D. C.-J., 2003, ApJS, 145, 259
Hodierno G., 1654, De systemate orbis cometici, deque admirandis coeli characteribus. typis Nicolai Bua, Panormi
Hubble E. P., 1926, ApJ, 63, 236
Hubble E., Sandage A., 1953, ApJ, 118, 353
Immler S., Swift Satellite Team, 2008, in Am. Astron. Soc. High-Energy Astrophysics Division, Meeting #10. Los Angeles, p. 07.05
Ivanov G. R., Freedman W. L., Madore B. F., 1993, ApJS, 89, 85
Jelinsky P. N. et al., 2003, in Blades J. C., Siegmund O. H. W., eds, Proc. SPIE Conf. Ser. Vol. 4854, Future EUV/UV and Visible Space Astrophysics Missions and Instrumentation. SPIE, Bellingham, p. 233

Kunchev P. Z., Ivanov G. R., 1986, Ap&SS, 122, 235
Landsman W. B., Roberts M. S., Bohlin R. C., O'Connell R. W., Smith A. M., Stecher T. P., 1992, ApJ, 401, L83
Lang D., Hogg D. W., Mierle K., Blanton M., Roweis S., 2012, Astrophysics Source Code Library, record ascl:1208.001
Long K. S., Dodorico S., Charles P. A., Dopita M. A., 1981, ApJ, 246, L61
Long K. S. et al., 2010, ApJS, 187, 495
Macri L. M., Sasselov D. D., Stanek K. Z., 2001, ApJ, 550, L159
Martin C., GALEX Science Team, 2003, BAAS, 35, 1363
Massey P., Bianchi L., Hutchings J. B., Stecher T. P., 1996, ApJ, 469, 629
Massey P., Olsen K. A. G., Hodge P. W., Strong S. B., Jacoby G. H., Schlingman W., Smith R. C., 2006, AJ, 131, 2478
Messier C., 1781, Tech. Rep. Catalogue des Nebuleuses and des amas d'Etoiles (Catalog of Nebulae and Star Clusters), Gauthier-Villars, Paris, France
Morrissey P. et al., 2007, ApJS, 173, 682
Neugent K. F., Massey P., 2011, ApJ, 733, 123
Pietsch W., Misanovic Z., Haberl F., Hatzidimitriou D., Ehle M., Trinchieri G., 2004, A&A, 426, 11
Romano G., 1978, Inf. Bull. Var. Stars, 1433, 1
Skrutskie M. F. et al., 2006, AJ, 131, 1163
Stecher T. P. et al., 1992, ApJ, 395, L1
Stetson P. B., 1987, PASP, 99, 191
Thilker D. A. et al., 2005, ApJ, 619, L67
Thompson T. A., Prieto J. L., Stanek K. Z., Kistler M. D., Beacom J. F., Kochanek C. S., 2009, ApJ, 705, 1364
Warner P. J., Wright M. C. H., Baldwin J. E., 1973, MNRAS, 163, 163

SUPPORTING INFORMATION

Additional Supporting Information may be found in the online version of this paper:

Table S1. UIT sources that were recovered using *GALEX* data. Here, 'Matches' refers to the number of *GALEX* objects we find that are within 5 arcsec and compatible with the given UIT source.
Table S2. Our UV sources that had optical counterparts from the LGGS. Note that all magnitudes are in the AB system. Here, 'Matches' refers to the number of optical objects we find that are within 3.2 arcsec of the *GALEX* source.
Table S3. Those UV sources that did not have an optical counterpart. Here, $N_{\rm mat}$ refers to the number of NUV sources within 3.2 arcsec of the FUV source.
(http://mnras.oxfordjournals.org/lookup/suppl/doi:10.1093/mnras/stv834/-/DC1).

Please note: Oxford University Press is not responsible for the content or functionality of any supporting materials supplied by the authors. Any queries (other than missing material) should be directed to the corresponding author for the paper.

This paper has been typeset from a TEX/LATEX file prepared by the author.